

Boundary renormalisation group flows of unitary superconformal minimal models

Márton Kormos*

*Institute for Theoretical Physics, Eötvös University,
1117 Budapest, Pázmány Péter sétány 1/A, Hungary*

December 20, 2018

Abstract

In this paper we investigate renormalisation group flows of supersymmetric minimal models generated by the boundary perturbing field $\hat{G}_{-1/2}\phi_{1,3}$. Performing the Truncated Conformal Space Approach analysis the emerging pattern of the flow structure is consistent with the theoretical expectations. According to the results, this pattern can be naturally extended to those cases for which the existing predictions are uncertain.

*kormos@general.elte.hu

1 Introduction

Conformal field theories with boundary attracted much interest recently, due to their relevance in condensed matter physics, e. g. in the Kondo problem [1] and their applications in describing D-branes in string theory [2, 3]. In terms of string theory the renormalisation group flow generated by a boundary perturbing field corresponds to tachyon condensation and exploring these flows can help in understanding the decay of D-branes.

Many papers appeared in the literature about the boundary perturbations and the corresponding renormalisation flows of unitary minimal models [4, 5, 6, 7, 8]. Up to now, a systematic charting of the boundary flows of the unitary *superconformal* minimal models has been missing. Although there may be flows within the perturbative domain, for a general study a nonperturbative tool is necessary. We choose the Truncated Conformal Space Approach (TCSA), originally proposed in the paper [9] and applied to boundary problems in [10] and [7]. The essence of the TCSA is to diagonalise the Hamiltonian of the system on a subspace of the infinite dimensional Hilbert space.

The paper is organised as follows. In section 2 we recall the basic facts that we need about superconformal minimal models, including the commutation rules of various fields. After briefly summarizing in section 3 some main properties of these models in the presence of boundaries, we turn to determining the Hamiltonian of the system and defining the boundary flows in section 4. We also motivate our choice for the perturbing operator in this section. Section 5 can be regarded as the main part of the paper: we introduce the TCSA method and give the details of the calculation of matrix elements. The theoretical expectations are briefly summarized in section 6, while our results are listed and compared to these expectations in section 7. Finally, in section 8 we summarize the conclusions of the paper. Some numerical data in tables and figures can be found in the Appendix.

2 Superconformal minimal models

2.1 The $N = 1$ superconformal algebra

The algebra of superconformal transformations in the plane are generated by two fields, $T(z)$ and $G(z)$ whose mode expansions read

$$T(z) = \sum_n L_n z^{-n-2}, \quad (2.1a)$$

$$G(z) = \sum_r G_r z^{-r-3/2}. \quad (2.1b)$$

$T(z)$ is a spin 2 field, while $G(z)$ has spin 3/2. Because of its fermionic character two kinds of boundary conditions are possible for $G(z)$:

$$G(e^{2\pi i} z) = G(z) \quad \rightarrow \text{Neveu-Schwarz sector}, \quad (2.2)$$

$$G(e^{2\pi i} z) = -G(z) \quad \rightarrow \text{Ramond sector}. \quad (2.3)$$

The $N = 1$ supersymmetric extension of the Virasoro algebra is defined by the following (anti)commutation relations:

$$[L_n, L_m] = (n - m)L_{n+m} + \frac{c}{12}n(n^2 - 1)\delta_{n,-m}, \quad (2.4a)$$

$$\{G_r, G_s\} = 2L_{r+s} + \frac{c}{3}(r^2 - 1/4)\delta_{r,-s}, \quad (2.4b)$$

$$[L_n, G_r] = \left(\frac{n}{2} - r\right)G_{n+r}. \quad (2.4c)$$

Here n, m denote integers, while according to the boundary conditions for $G(z)$ the indices r, s can take half-integer (Neveu-Schwarz sector) or integer (Ramond sector) values.

The highest weight representations of the algebra are defined by highest weight states $|h\rangle$ satisfying

$$L_n|h\rangle = 0 \quad n > 0, \quad (2.5a)$$

$$L_0|h\rangle = h, \quad (2.5b)$$

$$G_r|h\rangle = 0 \quad r > 0. \quad (2.5c)$$

The Verma module is generated by operators having a nonpositive index. The vectors

$$L_{n_1} \dots L_{n_k} G_{r_1} \dots G_{r_l} |h\rangle, \quad n_1 \leq \dots \leq n_k < 0, \quad r_1 < \dots < r_l \leq 0$$

constitute a basis for the Verma module. Note that the inequalities for the r_i -s are strict since $G_r^2 = L_{2r} - \frac{c}{12}\delta_{r,0}$ by equation (2.4b).

The full operator algebra of the Neveu-Schwarz and Ramond primary fields is nonlocal. However, there exist projections that give local operator algebras. One of

them is the so-called fermion model, in which one keeps only the Neveu–Schwarz sector.

In this paper we consider the so-called spin model which is obtained in the following way. In both sectors a fermion parity operator Γ can be introduced with algebraic relations $[\Gamma, L_n] = \{\Gamma, G_r\} = 0$. Thus every level of a Verma module consists of $\Gamma = \pm 1$ eigenstates. The projection onto the even parity ($\Gamma = +1$) states in the Neveu–Schwarz sector and onto either the even ($\Gamma = +1$) or the odd ($\Gamma = -1$) parity states in the Ramond sector yields a well defined local theory.

2.2 The minimal series

The irreducible highest weight representations are the quotients of the Verma modules by their maximal invariant submodules. In this paper we deal with the superconformal minimal models which contain only a finite number of Verma modules. In these models the Verma modules turn out to be highly reducible. The superconformal minimal models are indexed by two positive integers, p and q (we choose the convention $p < q$). Their central charge is given by

$$c(p, q) = \frac{3}{2} \left(1 - 2 \frac{(p - q)^2}{pq} \right), \quad \left(p, \frac{q - p}{2} \right) = 1. \quad (2.6)$$

Within a superconformal minimal model the highest weights are also characterized by two integers, r and s :

$$h(r, s) = \frac{(ps - qr)^2 - (p - q)^2}{8pq} + \frac{1 - (-1)^{r+s}}{32}, \quad 1 \leq r \leq p - 1, \quad 1 \leq s \leq q - 1. \quad (2.7)$$

The sum $r + s$ is even for a Neveu–Schwarz state and odd for a Ramond state. Setting $q = p + 2$ gives the one parameter family of *unitary* superconformal minimal models.

The fusion rule for the supersymmetric minimal models is

$$\phi_{(r_1, s_1)} \otimes \phi_{(r_2, s_2)} = \sum_{r' = |r_1 - r_2| + 1}^{\min \left(\frac{2p - r_1 - r_2 - 1}{r_1 + r_2 - 1} \right)} \sum_{s' = |s_1 - s_2| + 1}^{\min \left(\frac{2q - s_1 - s_2 - 1}{s_1 + s_2 - 1} \right)} \phi_{(r', s')}, \quad (2.8)$$

where the prime on the sums means that r' and s' jump by steps of 2. Since no field can appear on the right hand side more than once, the fusion rule coefficients are 1 for the fields appearing on the right hand side and 0 otherwise.

2.3 Field representations

Since we will be interested in correlation functions, we have to investigate how fields transform. Our discussion follows reference [11]. We denote the field corresponding to the state $|h\rangle$ by $\phi_h(z)$. By definition $\phi_h(z)|0\rangle = \exp(zL_{-1})|h\rangle$, where $|0\rangle$ is the superconform invariant vacuum state.

2.3.1 Virasoro properties

The mode expansion (2.1a) and the defining relations (2.5a, 2.5b) lead to the following operator product expansion:

$$T(z)\phi(w) = \frac{h\phi(w)}{(z-w)^2} + \frac{\partial\phi(w)}{z-w} + \dots \quad (2.9)$$

Using standard contour integration technique one obtains the commutation relation

$$L_n\phi(z) = z^n[(n+1)h + z\partial]\phi(z) + \phi(z)L_n. \quad (2.10)$$

Combining the relations for $n = m$ and $n = 0$ one arrives at

$$[L_m - z^m L_0, \phi(z)] = hmz^m\phi(z). \quad (2.11)$$

2.3.2 Neveu–Schwarz case

From equations (2.1b), (2.5c) and (2.4b) we conclude

$$G(z)\phi(w) = \frac{(\hat{G}_{-1/2}\phi)(w)}{z-w} + \dots, \quad (2.12a)$$

$$G(z)(\hat{G}_{-1/2}\phi)(w) = \frac{2h\phi(w)}{(z-w)^2} + \frac{\partial\phi(w)}{z-w} + \dots, \quad (2.12b)$$

where $\lim_{z \rightarrow 0}(\hat{G}_{-1/2}\phi)(z) = G_{-1/2}|h\rangle$.

The commutation relations in this case turn out to be

$$G_r\phi(z) = z^{r+1/2}(\hat{G}_{-1/2}\phi)(z) + \eta_\phi\phi(z)G_r, \quad (2.13a)$$

$$G_r(\hat{G}_{-1/2}\phi)(z) = z^{r-1/2}((2r+1)h + z\partial)\phi(z) - \eta_\phi(\hat{G}_{-1/2}\phi)(z)G_r \quad (2.13b)$$

with $\eta_\phi = \pm 1$ for fields of even and odd fermion number, respectively.

2.3.3 Ramond case

There is a cut in the operator product of $G(z)$ and a Ramond field and thus a Ramond field changes the moding of $G(z)$ from integral to half-integral and vice versa. So it is impossible to obtain a commutation relation of G_r with a Ramond field for fixed r . Fortunately, we can avoid using any (anti)commutation relation for Ramond fields in our calculations. All we need is formally generalizing relations (2.13) for integral r . Then, just like in the Virasoro case in section 2.3.1, combining the (2.13b) equations for $r = m$ and $r = 0$ yields

$$\begin{aligned} G_m(\hat{G}_{-1/2}\phi)(z) &= z^m G_0(\hat{G}_{-1/2}\phi)(z) + 2mh z^{m-1/2}\phi(z) \\ &\quad + \eta_\phi(\hat{G}_{-1/2}\phi)(z)(z^m G_0 - G_m). \end{aligned} \quad (2.14)$$

We will come back to these issues later in section 5.2.1.

3 Superconformal field theory on the upper half plane

The upper half plane (UHP) is the prototype of geometries having nontrivial boundaries. The superconformal transformations then have two roles. Firstly they connect the correlation functions on general geometries to those on the UHP. On the other hand the transformations that leave the geometry invariant put constraints on the correlation functions on the UHP.

In the following we give a lightning review of the superconformal boundary conditions and consistent boundary states based on paper [12].

The derivation of the Ward identity on the UHP leads to a new constraint on the operators of the chiral algebra. For the ordinary stress energy tensor one obtains $T_{xy}(x, 0) = 0$, which means that there is no energy flow across the boundary (the real axis). In complex coordinates this translates to the condition

$$T(z, \bar{z}) = \bar{T}(\bar{z}, z) \quad \text{for } \text{Re } z = 0. \quad (3.1)$$

A strip of width L with boundary conditions α and β on the left and the right boundary, respectively, can be mapped to the UHP by the exponential mapping, under which the boundaries of the strip are mapped to the negative and positive part of the real axis. The boundary conditions on the strip become conformal boundary conditions on the plane. The discontinuity of the boundary condition along the real axis can be described by a boundary condition changing field ψ^{ab} . These fields are in one to one correspondence with the operator content of the theory on the strip.

Looking at the strip from the side (“closed channel”) and letting the time flow in the direction of L the boundary conditions turn into initial and final boundary states. Then the conformal invariance of the boundary conditions translate to the following condition on these boundary states:

$$(L_n - \bar{L}_{-n})|B\rangle = 0 \quad (B = \alpha, \beta). \quad (3.2)$$

For a general chiral field W of spin s one finds

$$(W_n - (-1)^s \bar{W}_{-n})|B\rangle = 0, \quad (3.3)$$

which in our case means

$$(G_r \pm i\bar{G}_{-r})|B\rangle = 0. \quad (3.4)$$

This implies that the left-chiral and right-chiral part of the theory are linked together. Only one copy of the supersymmetric Virasoro algebra remains and all the calculations are chiral. It is also necessary to carry out the projection described in section 2.1.

The equations for the state $|B\rangle$ are solved in terms of the so-called Ishibashi states [13], whose linear combinations give the physically consistent boundary states. The further constraints for these states, generalizations of the Cardy-equations [14], come from the modular properties of the partition function.

Now let us list the main results of this analysis. In the Ramond sector the consistent boundary states are in one-to-one correspondence with the irreducible highest weight representations of the algebra, so they can be labeled by the same index set: we will denote them by $|\mathbf{k}^R\rangle$. In the Neveu–Schwarz sector there are two physical boundary states for every irreducible representation, they are denoted by $|\mathbf{k}^{\text{NS}}\rangle$ and $|\mathbf{k}^{\widetilde{\text{NS}}}\rangle$.

For the $\text{SM}(p, p+2)$ models (with p odd) the state content of the Hilbert space of the theory on the strip with boundary conditions α and β is given by

$$\text{tr}_{\text{NS}} e^{-RH_{\alpha\beta}} = \sum_{i \in \Delta_{\text{NS}}} n_{\alpha\beta}^i \chi_i^{\text{NS}}(q), \quad (3.5a)$$

$$\text{tr}_{\text{NS}} \Gamma e^{-RH_{\alpha\beta}} = \sum_{i \in \Delta_{\text{NS}}} \tilde{n}_{\alpha\beta}^i \chi_i^{\widetilde{\text{NS}}}(q), \quad (3.5b)$$

$$\text{tr}_{\text{R}} e^{-RH_{\alpha\beta}} = \sum_{i \in \Delta_{\text{R}}} m_{\alpha\beta}^i \chi_i^{\text{R}}(q), \quad (3.5c)$$

$$\text{tr}_{\text{R}} \Gamma e^{-RH_{\alpha\beta}} = 0, \quad (3.5d)$$

where $q = e^{-\pi R/L}$ and the characters are

$$\chi_i^{\text{NS}}(q) = \text{tr}_i q^{L_0 - c/24}, \quad i \in \Delta_{\text{NS}}, \quad (3.6a)$$

$$\chi_i^{\widetilde{\text{NS}}}(q) = \text{tr}_i \Gamma q^{L_0 - c/24}, \quad i \in \Delta_{\text{NS}}, \quad (3.6b)$$

$$\chi_i^{\text{R}}(q) = \text{tr}_i q^{L_0 - c/24}, \quad i \in \Delta_{\text{R}}. \quad (3.6c)$$

Using a generalised Verlinde formula the coefficients $n_{\alpha\beta}^i$ and $m_{\alpha\beta}^i$ can be identified with the fusion rule coefficients in the fusion $\Phi_\alpha \times \Phi_\beta \rightarrow \Phi_i$. Particularly,

$$n_{\mathbf{0}_{\text{NS}} \mathbf{k}_{\text{NS}}}^i = \tilde{n}_{\mathbf{0}_{\text{NS}} \mathbf{k}_{\text{NS}}}^i = \delta_k^i, \quad m_{\mathbf{0}_{\text{NS}} \mathbf{k}_{\text{NS}}}^i = 0, \quad (3.7a)$$

$$n_{\mathbf{0}_{\text{NS}} \mathbf{k}_{\widetilde{\text{NS}}}}^i = -\tilde{n}_{\mathbf{0}_{\text{NS}} \mathbf{k}_{\widetilde{\text{NS}}}}^i = \delta_k^i, \quad m_{\mathbf{0}_{\text{NS}} \mathbf{k}_{\widetilde{\text{NS}}}}^i = 0, \quad (3.7b)$$

$$n_{\mathbf{0}_{\text{NS}} \mathbf{k}_{\text{R}}}^i = \tilde{n}_{\mathbf{0}_{\text{NS}} \mathbf{k}_{\text{R}}}^i = 0, \quad m_{\mathbf{0}_{\text{NS}} \mathbf{k}_{\text{R}}}^i = 2\delta_k^i. \quad (3.7c)$$

The field content of the (projected) theory is thus given by

$$Z = \text{tr}_{\text{NS}} \frac{1}{2} (1 + \Gamma) e^{-RH_{\alpha\beta}} + \text{tr}_{\text{R}} \frac{1}{2} (1 + \Gamma) e^{-RH_{\alpha\beta}} = \frac{1}{2} \sum_{i \in \Delta_{\text{NS}}} \left(n_{\alpha\beta}^i \chi_i^{\text{NS}}(q) + \tilde{n}_{\alpha\beta}^i \chi_i^{\widetilde{\text{NS}}}(q) \right) + \frac{1}{2} \sum_{i \in \Delta_{\text{R}}} m_{\alpha\beta}^i \chi_i^{\text{R}}(q). \quad (3.8)$$

If we choose β corresponding to $|\mathbf{0}^{\text{NS}}\rangle$ and α to $|\mathbf{k}^{\text{NS}}\rangle$ (or $|\mathbf{0}^{\widetilde{\text{NS}}}\rangle$ and $|\mathbf{k}^{\widetilde{\text{NS}}}\rangle$) then the right hand side becomes

$$Z = \frac{1}{2} \left(\chi_k^{\text{NS}}(q) + \chi_k^{\widetilde{\text{NS}}}(q) \right) = \text{tr}_{\mathbf{k}}^{\text{NS}} \frac{1}{2} (1 + \Gamma) q^{L_0 - c/24}. \quad (3.9)$$

In case we choose β corresponding to $|\mathbf{0}^{\text{NS}}\rangle$ and α to $|\mathbf{k}^{\widetilde{\text{NS}}}\rangle$ (or $|\mathbf{0}^{\widetilde{\text{NS}}}\rangle$ and $|\mathbf{k}^{\text{NS}}\rangle$) we get

$$Z = \frac{1}{2} \left(\chi_k^{\text{NS}}(q) - \chi_k^{\widetilde{\text{NS}}}(q) \right) = \text{tr}_k^{\text{NS}} \frac{1}{2} (1 - \Gamma) q^{L_0 - c/24}. \quad (3.10)$$

Finally, if we choose β corresponding to $|\mathbf{0}^{\text{NS}}\rangle$ (or $|\mathbf{0}^{\widetilde{\text{NS}}}\rangle$) and α to $|\mathbf{k}^{\text{R}}\rangle$ the result is

$$Z = \chi_k^{\text{R}}(q). \quad (3.11)$$

The case of even p is more complicated due to the special supersymmetric representation $(\frac{p}{2}, \frac{p+2}{2})$.

4 Boundary renormalisation group flows

In this paper we examine RG flows of superconformal minimal models with boundary, generated by a boundary field. Since no bulk perturbing field is allowed and the boundary perturbation preserves supersymmetry, the RG flow takes place in the space of possible supersymmetric boundary conditions, in which the fixed points are the superconformal ones.

To study flows starting from a Cardy boundary condition it is convenient to choose the boundary condition on one of the edges of the strip to correspond to the $h = 0$ primary field, that is $\beta \sim |\mathbf{0}^{\text{NS}}\rangle$ or $|\mathbf{0}^{\widetilde{\text{NS}}}\rangle$. Then (3.9) implies that if α and β are both NS or $\widetilde{\text{NS}}$ type boundary conditions, the Hilbert space contains only the bosonic half of a single Neveu–Schwarz module, the one corresponding to α . Similarly, according to (3.10), if α is a NS type and β is a $\widetilde{\text{NS}}$ type boundary condition (or vice versa), the Hilbert space consists of the fermionic half of a single α module. Finally, as (3.11) shows, if α is a R type boundary condition, the Hilbert space contains a single Ramond module.

At the endpoint of the flow the final boundary condition can be read off in a similar way simply from the spectrum of the Hamiltonian. Since the boundary condition β does not change along the flow (it is not perturbed), if we start with the bosonic half of a NS Verma module (NS–NS or $\widetilde{\text{NS}}\text{--}\widetilde{\text{NS}}$) and at the end of the flow we find bosonic part(s) of Verma module(s) then this is a NS \rightarrow NS (or $\widetilde{\text{NS}} \rightarrow \widetilde{\text{NS}}$) type flow. Similarly, if we identify fermionic part(s) then this indicates a NS \rightarrow $\widetilde{\text{NS}}$ (or $\widetilde{\text{NS}} \rightarrow$ NS) type flow.

We have to choose the perturbing field on the boundary α . We would like a perturbation that preserves supersymmetry off-critically. Ramond operators do not spoil supersymmetry but they are boundary condition changing operators, so they cannot live on a boundary. Neveu–Schwarz fields of the form $(\hat{G}_{-1/2}\phi_{\text{pert}})$ also preserve supersymmetry and they can be located on the boundary, so we choose this kind of perturbation. The perturbing operator should be relevant, that is its scaling dimension must be less than one. Finally, since the Hamiltonian is bosonic, ϕ_{pert} must be fermionic. The choice $\phi_{\text{pert}} = \phi_{1,3}$ satisfy all these conditions. $(\hat{G}_{-1/2}\phi_{1,3})$

has conformal weight $p/q < 1$ and $\phi_{1,3}$ is fermionic. The latter can be seen from the fact that in the free fermion limit $p, q \rightarrow \infty$ ($q - p = \text{const.}$) $h_{1,3} \rightarrow 1/2$.

Our choice also has the advantage that this operator can live on every boundary that has supersymmetric relevant perturbations. This can be seen from the following. An operator ψ living on the boundary of the strip is mapped under the exponential map to an operator living on the real axis. We want this operator to leave the boundary condition unchanged along the axis, which means that the coefficients in (3.5) for $\alpha = \beta$ should be nonzero. Since they can be related to the fusion coefficients this means that the representation h_ψ should appear in the fusion of ϕ_α with itself¹. The field $\phi_{1,3}$ appears in the self fusion of all fields except for the ones in the first and the last column of the superconformal Kac table ($\phi_{(1,s)}, \phi_{(p-1,s)}$), but the corresponding boundaries do not have any relevant supersymmetric perturbations at all. Also note that being a bosonic field, the fusion with $(\hat{G}_{-1/2}\phi_{1,3})$ maps the projected subspaces onto themselves.

The perturbation $(\hat{G}_{-1/2}\phi_{1,3})$ is an integrable one [15], but we shall not use this property in our analysis.

The Hamiltonian of the perturbed superconformal field theory takes the form

$$H = H_{\text{CFT}} + H_{\text{pert}} , \quad (4.1)$$

where H_{CFT} is the Hamiltonian of the unperturbed theory

$$H_{\text{CFT}} = H_{\alpha 0} = \frac{\pi}{L} \left(L_0 - \frac{c}{24} \right) \quad (4.2)$$

and H_{pert} comes from the perturbation on the strip:

$$H_{\text{pert}}^{\text{strip}} = \lambda (\hat{G}_{-1/2}\phi_{1,3})(0, 0) . \quad (4.3)$$

The location of the left boundary is at $x = 0$ and we are free to choose $t = 0$ for calculating the spectrum. By the exponential map this on the z -plane becomes

$$H_{\text{pert}} = \lambda \left(\frac{\pi}{L} \right)^{h_{1,3}+1/2} (\hat{G}_{-1/2}\phi_{1,3})(1)_z . \quad (4.4)$$

Thus the complete Hamiltonian on the plane can be written as

$$H = \frac{\pi}{L} \left[L_0 - \frac{c}{24} + \lambda \left(\frac{L}{\pi} \right)^{1/2-h_{1,3}} (\hat{G}_{-1/2}\phi_{1,3})(1) \right] . \quad (4.5)$$

Since during a numerical calculation one works with dimensionless quantities we have to measure the volume (L) and the energies in some typical mass or energy

¹The coefficients $\tilde{n}_{\alpha\beta}^i$ are not fusion coefficients themselves, but this does not change the argument essentially.

difference of the model, M . In other words, we use the dimensionless quantities $l = ML$, $\varepsilon = E/M$, $\kappa = \lambda/M^{1/2-h_{1,3}}$ and $h = H/M$:

$$h = \frac{\pi}{l} \left[L_0 - \frac{c}{24} + \kappa \left(\frac{l}{\pi} \right)^{1/2-h_{1,3}} (\hat{G}_{-1/2}\phi_{1,3})(1) \right]. \quad (4.6)$$

The renormalisation group flow can be implemented by varying the volume l while keeping the coupling constant κ fixed. Equivalently – and we choose this way – one can keep l fixed and vary κ on some interval. Starting from $\kappa = 0$, which is the ultraviolet (UV) limit, the matrix h can be diagonalised at different positive and negative values of κ . In both directions the flow approaches a fixed point, that is a new supersymmetric conformal boundary condition. By (3.5) we should observe the eigenstates rearranging themselves into a direct sum of super Verma modules (see the figures in the Appendix). Since by (3.7) the coefficients in this sum can only take values 0 and 1, we expect a simple sum of super Verma modules at the end of the flows. From the degeneracy pattern of the eigenvalues we can identify the modules (the boundary conditions) using the characters and weight differences of the supersymmetric minimal model in question.

5 The Truncated Conformal Space Approach

The method we use for organising the boundary flows is the so-called truncated conformal space approach, or TCSA. In this approach the infinite dimensional Hilbert space is truncated to a finite dimensional vector space by using only those states whose energy is not greater than a threshold value, E_{cut} . This is equivalent to truncating the Hilbert space at a given level. The Hamiltonian is then diagonalised on this truncated space. One can think of this procedure as being equivalent to the variational method: the Ansatzes for the energy eigenstates of the perturbed Hamiltonian are finite linear combinations of the eigenstates of the conformal Hamiltonian.

It is important that the errors of the TCSA diagonalisation are not under control. For example, it may happen that before the flow reaches the scaling region the truncation errors start to dominate. If we use various cuts and find that the flow picture does not change drastically (only the precision of the result gets higher with higher cuts), then it means that the unpleasant case mentioned above does not happen.

Of course establishing the endpoint of the renormalisation group flow by TCSA cannot be regarded as a conclusive proof. What one can see is that the flow goes in the vicinity of some superconformal boundary condition. The exact infrared fixed point can never be reached by TCSA because of the truncation (this can be observed in figure 3(a)). We are looking for the range where the TCSA trajectory is closest to the fixed point.

5.1 The matrix elements of the Hamiltonian

There are two ways for determining the eigenvalues of the total Hamiltonian. The first is to use an orthonormal basis for calculating the matrix elements, which requires an orthogonalisation process. We can avoid this by choosing the second way, in which the basis is not orthonormal. But then the numerical matrix to be diagonalised is

$$h_{ij} = \langle f_i | h | e_j \rangle, \quad (5.1)$$

where $\{f_i\}$ are the elements of the reciprocal basis, that is

$$\langle f_i | e_j \rangle = \delta_{ij}. \quad (5.2)$$

This amounts to calculating the matrix element

$$h_{ij} = (M^{-1})_{ik} \langle e_k | h | e_j \rangle, \quad (5.3)$$

where M is the inner product matrix:

$$M_{ij} = \langle e_i | e_j \rangle. \quad (5.4)$$

Using the notation

$$B_{ij} = \langle e_i | (\hat{G}_{-1/2} \phi_{1,3})(1) | e_j \rangle \quad (5.5)$$

it can be expressed as

$$h_{ij} = \frac{\pi}{l} \left[\left(h_i - \frac{c}{24} \right) \delta_{ij} + \kappa \left(\frac{l}{\pi} \right)^{1/2 - h_{1,3}} (M^{-1} B)_{ij} \right]. \quad (5.6)$$

Here we made use of the fact that the basis elements $\{e_i\}$ are eigenvectors of H_0 .

5.2 Computing the matrix elements of the perturbing field between descendant states

The task is now to calculate the matrices M and B and then to determine the eigenvalues of the resulting matrix h . The Hilbert space consists of the Verma module of ϕ_α (see eq. (3.5)) and as mentioned above, we choose the following basis elements:

$$L_{n_1} \dots L_{n_k} G_{r_1} \dots G_{r_l} |h\rangle, \quad n_1 \leq \dots \leq n_k < 0, \quad r_1 < \dots < r_l \leq 0. \quad (5.7)$$

Due to the singular vectors, not all of these are linearly independent. One can obtain a basis for the irreducible submodule by requiring the nonsingularity of the inner product matrix level by level. In the Ramond sector we kept the states which had even number of G_r operators. Choosing the odd parity sector instead gives exactly the same result: the spectrum of the Hamiltonian falls into two identical copies.

The calculation of h is now a question of algebraic manipulations. We use the basic algebraic relations (2.4), (2.5) and the definition of adjoint operators

$$L_n^\dagger = L_{-n} , \quad (5.8)$$

$$G_n^\dagger = G_{-n} . \quad (5.9)$$

In the Ramond case during the calculation of the inner product matrix M we also demand that $\langle \alpha | G_0 | \beta \rangle = 0$ (α and β are primary), because the inner product of states with opposite Γ -parity must vanish.

The calculation of the matrix B is more difficult because it requires the usage of some commutation rules for reducing the matrix elements. However, these commutation rules are different for the Ramond and the Neveu–Schwarz case. Let us deal with the two cases in turn.

5.2.1 Ramond case

In the Ramond case we can use the already mentioned commutational rules (2.11), (2.13a) and (2.14). We recall them because they lie at the heart of the algorithm. For the modes L_n we saw (cf. (2.11))

$$L_n \phi(z) = z^n L_0 \phi(z) + \phi(z)(n h z^n - z^n L_0 + L_n) , \quad (5.10a)$$

$$\phi(z) L_n = z^n \phi(z) L_0 + (-n h z^n - z^n L_0 + L_n) \phi(z) . \quad (5.10b)$$

Similarly

$$\begin{aligned} L_n(\hat{G}_{-1/2}\phi)(z) &= z^n L_0(\hat{G}_{-1/2}\phi)(z) \\ &\quad + (\hat{G}_{-1/2}\phi)(z)(n(h + 1/2)z^n - z^n L_0 + L_n) , \end{aligned} \quad (5.11a)$$

$$\begin{aligned} (\hat{G}_{-1/2}\phi)(z) L_n &= z^n (\hat{G}_{-1/2}\phi)(z) L_0 \\ &\quad + (-n(h + 1/2)z^n - z^n L_0 + L_n)(\hat{G}_{-1/2}\phi)(z) . \end{aligned} \quad (5.11b)$$

We make use of these formulae in reducing the three point functions. Here is an example of the application of rule (5.10a):

$$\begin{aligned} \langle L_{-n} \mathcal{O}_1 \alpha | \phi_{1,3}(1) | \mathcal{O}_2 \alpha \rangle &= \langle \mathcal{O}_1 \alpha | L_n \phi_{1,3}(1) | \mathcal{O}_2 \alpha \rangle \\ &= (h_\alpha + n h_{1,3} - h_\alpha) \langle \mathcal{O}_1 \alpha | \phi_{1,3}(1) | \mathcal{O}_2 \alpha \rangle + \langle \mathcal{O}_1 \alpha | \phi_{1,3}(1) | L_n \mathcal{O}_2 \alpha \rangle , \end{aligned} \quad (5.12)$$

where \mathcal{O}_1 and \mathcal{O}_2 are arbitrary strings of lowering operators.

The counterpart of these relations for the modes G_r are (see (2.13a))

$$G_r \phi(z) = z^{r+1/2}(\hat{G}_{-1/2}\phi)(z) + \eta_\phi \phi(z) G_r , \quad (5.13a)$$

$$\phi(z) G_r = -\eta_\phi z^{r+1/2}(\hat{G}_{-1/2}\phi)(z) + \eta_\phi G_r \phi(z) , \quad (5.13b)$$

and (cf. (2.14))

$$G_m(\hat{G}_{-1/2}\phi)(z) = z^m G_0(\hat{G}_{-1/2}\phi)(z) + 2mh z^{m-1/2} \phi(z) + \eta_\phi(\hat{G}_{-1/2}\phi)(z)(z^m G_0 - G_m), \quad (5.14a)$$

$$(\hat{G}_{-1/2}\phi)(z)G_m = z^m(\hat{G}_{-1/2}\phi)(z)G_0 + \eta_\phi 2mh z^{m-1/2} \phi(z) + \eta_\phi(z^m G_0 - G_m)(\hat{G}_{-1/2}\phi)(z). \quad (5.14b)$$

These rules can be used in a similar way to (5.12), but only if ϕ_α is a Ramond field ($G_0\phi_\alpha$ is not defined for Neveu–Schwarz fields). Iteratively applying the rules (5.11) and (5.13), (5.14) to a matrix element leads to a linear combination of the following correlation functions:

$$\langle \alpha | (\hat{G}_{-1/2}\phi_{1,3})(1) | \alpha \rangle, \quad (5.15a)$$

$$\langle \alpha | \phi_{1,3}(1) | \alpha \rangle, \quad (5.15b)$$

$$\langle G_0\alpha | \phi_{1,3}(1) | \alpha \rangle, \quad (5.15c)$$

$$\langle \alpha | \phi_{1,3}(1) | G_0\alpha \rangle. \quad (5.15d)$$

The second of these always equals to zero in our case, because $\phi_{1,3}$ is a fermion-like operator. This also means that $\eta_{\phi_{1,3}} = -1$.

Due to (5.13a)

$$\langle G_0\alpha | \phi_{1,3}(1) | \alpha \rangle = \langle \alpha | (\hat{G}_{-1/2}\phi_{1,3})(1) | \alpha \rangle + \eta_\phi \langle \alpha | \phi_{1,3}(1) | G_0\alpha \rangle. \quad (5.16)$$

Since $G_0^\dagger = G_0$

$$\langle G_0\alpha | \phi_{1,3}(1) | \alpha \rangle = \langle \alpha | \phi_{1,3}(1) | G_0\alpha \rangle, \quad (5.17)$$

which implies for $\eta_{\phi_{1,3}} = -1$

$$\langle G_0\alpha | \phi_{1,3}(1) | \alpha \rangle = \frac{1}{2} \langle \alpha | (\hat{G}_{-1/2}\phi_{1,3})(1) | \alpha \rangle. \quad (5.18)$$

We see that every matrix element can be traced back to the three point function

$$\langle \alpha | (\hat{G}_{-1/2}\phi_{1,3})(1) | \alpha \rangle = \langle \phi_\alpha(\infty), (\hat{G}_{-1/2}\phi_{1,3})(1), \phi_\alpha(0) \rangle \quad (5.19)$$

which simply equals to a structure constant. However, we do not need the numerical value of this constant, because it can be absorbed into the coupling constant κ . The physical scale is fixed by the value of κ where the crossover takes place. Since we are interested only in the asymptotic behaviour of the flows (the fixed points), we do not need to fix the real physical scale.

5.2.2 Neveu–Schwarz case

In the Neveu–Schwarz case we can derive the rules for reducing the three point functions using contour integration technique. From

$$\begin{aligned}\langle L_n A(\infty) | B(0) \rangle &= \langle A(\infty) | L_{-n} B(0) \rangle = \langle A(\infty) | \oint_0 \frac{dz}{2\pi i} z^{-n+1} T(z) B(0) \rangle \\ &= \langle - \oint_\infty \frac{dz}{2\pi i} z^{-n+1} T(z) A(\infty) | B(0) \rangle\end{aligned}\quad (5.20)$$

we obtain

$$L_n \Phi(\infty) = - \oint_\infty \frac{dz}{2\pi i} z^{-n+1} T(z) \Phi(\infty). \quad (5.21)$$

Then for a three point function:

$$\begin{aligned}\langle L_{-n} A(\infty) | B(1) | C(0) \rangle &= - \oint_\infty \frac{dz}{2\pi i} z^{n+1} \langle T(z) A(\infty) | B(1) | C(0) \rangle \\ &= \oint_1 \frac{dz}{2\pi i} \sum_{k=-1}^n \binom{n+1}{k+1} (z-1)^{k+1} \langle A(\infty) | T(z) B(1) | C(0) \rangle \\ &\quad + \oint_0 \frac{dz}{2\pi i} z^{n+1} \langle A(\infty) | B(1) | T(z) C(0) \rangle \\ &= \langle A(\infty) | B(1) | L_n C(0) \rangle + \sum_{k=-1}^n \binom{n+1}{k+1} \langle A(\infty) | L_k B(1) | C(0) \rangle.\end{aligned}\quad (5.22)$$

With similar manipulations one can obtain rules for the remaining two initial positions of L_{-n} and their counterparts for the modes G_{-r} . These formulae can be obtained from the algebraic commutation relations as well. Now they can be applied iteratively to the three point function in the following manner.

First we throw down all operators from the first field to the others:

$$\langle L_{-n} A | B(1) | C \rangle = \langle A | B(1) | L_n C \rangle + \sum_{k=-1}^n \binom{n+1}{k+1} \langle A | L_k B(1) | C \rangle, \quad (5.23a)$$

$$\langle G_{-n} A | B(1) | C \rangle = \eta_B \langle A | B(1) | G_n C \rangle + \sum_{k=-1/2}^n \binom{n+\frac{1}{2}}{k+\frac{1}{2}} \langle A | G_k B(1) | C \rangle. \quad (5.23b)$$

Then, exploiting that A is now primary we throw everything from the rightmost

field to the middle one:

$$\langle A|B(1)|L_{-n}C\rangle = -\sum_{k=-1}^{\infty} \binom{-n+1}{k+1} \langle A|L_k B(1)|C\rangle, \quad (5.24a)$$

$$\langle A|B(1)|G_{-n}C\rangle = -\eta_B \sum_{k=-1/2}^{\infty} \binom{-n+\frac{1}{2}}{k+\frac{1}{2}} \langle A|G_k B(1)|C\rangle. \quad (5.24b)$$

Certainly, in practice the sums truncate at the level of B . Finally we eliminate the operators from the field B (A and C are now primary):

$$\langle A|L_{-n}B(1)|C\rangle = (-1)^n \langle A|B(1)|L_{-1}C\rangle + (-1)^n(n-1) \langle A|B(1)|L_0C\rangle, \quad (5.25a)$$

$$\langle A|G_{-n}B(1)|C\rangle = \eta_B(-1)^{n+1/2} \langle A|B(1)|G_{-1/2}C\rangle. \quad (5.25b)$$

Now we can throw this L_{-1} and $G_{-1/2}$ back onto the middle field using (5.24) and repeat step (5.25). Eventually some L_{-1} and possibly one $G_{-1/2}$ can accumulate on the middle field. The effect of operators L_{-1} is simply differentiating. Since conformal symmetry determines the functional form of the three point function of quasi-primary fields we obtain:

$$\begin{aligned} \langle A|L_{-1}^m B(1)|C\rangle &= (h_A - h_B - h_C)(h_A - h_B - h_C - 1) \dots \\ &\dots (h_A - h_B - h_C - m + 1) \langle A|B(1)|C\rangle. \end{aligned} \quad (5.26)$$

The final result is – like in the Ramond case – a linear combination of matrix elements (5.15a), (5.15b) where the second one gives zero again.

The reason for not using contour integral technique in the Ramond case is the presence of the cut in the operator product of $G(z)$ with a Ramond field.

It is interesting to note that albeit $G_0\phi_\alpha$ is not really well-defined for ϕ_α being a Neveu–Schwarz field, the Ramond method explained in section 5.2.1 still works in the Neveu–Schwarz case and gives the same result as the contour integral method.

6 Previous results and expectations

Before turning to the result of the TCSA let us summarize the theoretical predictions for the boundary flows found in the literature. Our main resource is the paper of Fredenhagen [16], where the author gives some predictions for boundary flows in general coset models. Here we only summarize the consequences for the special case of superconformal minimal models.

The $SM(p, p+2)$ unitary superminimal models are realized by the

$$\frac{su(2)_k \otimes su(2)_2}{su(2)_{k+2}} \quad (6.1)$$

coset models with $p = k+2$. Let us label the sectors of $su(2)_k$ by $l = 0, 1, \dots, k$, the sectors of $su(2)_2$ by $m = 0, 1, 2$ and the sectors of $su(2)_{k+2}$ by $l' = 0, 1, \dots, k+2$.

The sectors of the direct product are thus labeled by the pairs (l, m) . These sectors split up with respect to the $su(2)_{k+2}$ subalgebra,

$$V_{l,m} = \bigoplus_{l'} W_{l,m,l'} \otimes V_{l'}, \quad (6.2)$$

where $W_{l,m,l'}$ are the sectors of the coset theory. Only those coset sectors are allowed for which

$$l + m + l' \text{ is even.} \quad (6.3)$$

Furthermore, there are identifications between these admissible representations:

$$(l, m, l') \cong (k - l, 2 - m, k + 2 - l'). \quad (6.4)$$

Using the $p = k + 2$ rule and the new variables (the Kac-indices)

$$\begin{aligned} r &= l + 1 & r &= 1, 2, \dots, p - 1, \\ s &= l' + 1 & s &= 1, 2, \dots, p + 1 \end{aligned}$$

the precise relations with the superminimal fields are (see [17]):

$$(r, s)_{\text{NS}} = (r - 1, 0, s - 1) \oplus (r - 1, 2, s - 1), \quad (6.6)$$

$$(r, s)_{\text{R}} = (r - 1, 1, s - 1). \quad (6.7)$$

In the Neveu–Schwarz sector the direct sum in (6.6) corresponds to the sum of the Γ -projected subspaces. The identification (6.4) translates to

$$(r, s) \cong (p - r, p + 2 - s), \quad (6.8)$$

which is the well-known symmetry relation of the Kac table of the superminimal models.

In the A-series of superminimal models the boundary conditions α are labeled by triplets (l, m, l') taking values in the same range as the sectors including selection and identification rules. The NS and $\widetilde{\text{NS}}$ boundary conditions correspond to the $m = 0, 2$ choices. The agreement between our results and the predictions for the flows justifies this correspondence.

The boundary flows are predicted in the following way. First we have to find a boundary condition α and a representation S so that

$$(0, S^+|_{su(2)_{k+2}}) \times \alpha = (l, m, l'), \quad (l + m + l' \text{ is even}). \quad (6.9)$$

Then a boundary flow is predicted between the following coset boundary configurations:

$$X := (0, S^+|_{su(2)_{k+2}}) \times \alpha \longrightarrow (S, 0) \times \alpha =: Y. \quad (6.10)$$

If we want to study flows starting from the boundary condition (l, m, l') with $0 \leq l' \leq k$ we can set $\alpha = (l, m, 0)$ and $S = (l', 0)$. This choice corresponds to the flow

$$(l, m, l') \longrightarrow \bigoplus_J N_{l,l'}^{(k)J}(J, m, 0), \quad (6.11)$$

where the $N_{l,l'}^{(k)J}$ are the fusion coefficients in $su(2)_k$.

Similarly, in the case of $2 \leq l' \leq k+2$ the choice $\alpha = (k-l, 2-m, 0)$ and $S = (k+2-l', 0)$ leads to the flow

$$(l, m, l') \longrightarrow \bigoplus_J N_{l,l'-2}^{(k)J}(J, 2-m, 0). \quad (6.12)$$

The boundary conditions which are not covered by these rules are² for $l' = k+1, 1$. These correspond to the (r, p) and $(r, 2)$ states. (The boundary conditions $(r, p+1)$ and $(r, 1)$ do not have relevant supersymmetric perturbations.)

For $l' = k+1$ the suitable choice is $S = (0, 1)$ and $\alpha = (l, m, k+2)$. Then

$$(l, 0 \text{ or } 2, k+1) \longrightarrow (l, 1, k+2) \cong (k-l, 1, 0), \quad (6.13)$$

$$(l, 1, k+1) \longrightarrow (k-l, 0, 0) \oplus (k-l, 2, 0). \quad (6.14)$$

Finally, for $l' = 1$ one should choose $S = (0, 1)$ and $\alpha = (l, m, 0)$, which yields the flows

$$(l, 0 \text{ or } 2, 1) \longrightarrow (l, 1, 0), \quad (6.15)$$

$$(l, 1, 1) \longrightarrow (l, 0, 0) \oplus (l, 2, 0). \quad (6.16)$$

Let us summarize the $l = 0$ case, when these results give

$$(0, m, l') \longrightarrow (l', m, 0) \quad 0 \leq l' \leq k, \quad (6.17)$$

$$(0, 0 \text{ or } 2, k+1) \longrightarrow (k, 1, 0) \quad l' = k+1, \quad (6.18)$$

$$(0, 1, k+1) \longrightarrow (k, 0, 0) \oplus (k, 2, 0), \quad (6.19)$$

$$(0, m, l') \longrightarrow (l' - 2, 2 - m, 0) \quad 2 \leq l' \leq k+2, \quad (6.20)$$

$$(0, 1, 1) \longrightarrow (0, 0, 0) \oplus (0, 2, 0). \quad (6.21)$$

Multiplying both sides of these rules by $(l, 0, 0)$ we get back the rules for general l . In the Kac index language this is the „disorder line rule”, discussed in paper [18]: if there is a flow between boundary conditions α and β , then there exists a flow between $\alpha \times \gamma$ and $\beta \times \gamma$ where \times denotes the fusion product. For the boundary states of $N = 1$ superminimal models the fusion rule (2.8) should be used together with the rules³

$$\text{NS} \times \text{NS} = \widetilde{\text{NS}} \times \widetilde{\text{NS}} = \text{NS}, \quad (6.22a)$$

$$\text{NS} \times \widetilde{\text{NS}} = \widetilde{\text{NS}}, \quad (6.22b)$$

$$\text{R} \times \text{NS} = \text{R} \times \widetilde{\text{NS}} = \text{R}, \quad (6.22c)$$

$$\text{R} \times \text{R} = \text{NS} \oplus \widetilde{\text{NS}}. \quad (6.22d)$$

²The author is thankful to S. Fredenhagen for the private discussion on these cases.

³These are correct with the choice $m = 0 \iff \text{NS}$ and $m = 2 \iff \widetilde{\text{NS}}$. In case of the other choice a $\text{NS} \leftrightarrow \widetilde{\text{NS}}$ swap is needed.

This means that we only need to determine the flows starting from states in the first row of the Kac table, all the other flows are given by the fusion rules of the operator algebra.

The authors of paper [19] have also derived the flows for some Neveu–Schwarz states in the first row of the Kac table, but only for even p .

7 TCSA results

We were searching the answers for the following questions.

1. Does our TCSA analysis affirm or disprove the predictions of the Fredenhagen rules?
2. Do all the flows obey the disorder line rule?
3. What happens in the p even models, where both these rules and the classification of consistent boundary conditions are somewhat certain?

We have positive answers for the first two questions. Namely, the following rules can be read out from the TCSA analysis of the boundary flows of the unitary superconformal minimal model $\text{SM}(p, p+2)$ perturbed by the operator $\hat{G}_{-1/2}\phi_{1,3}$ (see also the Appendix):

1. For $\kappa > 0$:

- (a) For $2 \leq s \leq p-1$

$$(1, s)_{\text{NS}} \longrightarrow (s, 1)_{\text{NS}}, \quad (7.1a)$$

$$(1, s)_{\widetilde{\text{NS}}} \longrightarrow (s, 1)_{\widetilde{\text{NS}}}, \quad (7.1b)$$

$$(1, s)_{\text{R}} \longrightarrow (s, 1)_{\text{R}}. \quad (7.1c)$$

This agrees with the Fredenhagen result (6.17). According to the disorder line rule we found (cf. (6.11)):

$$(r, s) \rightarrow (|s-r|+1, 1) \oplus (|s-r|+3, 1) \oplus \cdots \oplus (\min(\frac{s+r-1}{2p-(s+r)-1}, 1), 1). \quad (7.2)$$

These flows do not change the type of the boundary condition so on the right hand side all the boundary conditions are of the same type. Thus, if two of them have different fermion parity, then the half-integer levels of one should combine with the integer levels of the other. That is exactly what we observed.

- (b) For $s = p$

$$(1, p)_{\text{NS}} \longrightarrow (p-1, 1)_{\text{R}}, \quad (7.3a)$$

$$(1, p)_{\widetilde{\text{NS}}} \longrightarrow (p-1, 1)_{\text{R}}, \quad (7.3b)$$

$$(1, p)_{\text{R}} \longrightarrow (p-1, 1)_{\text{NS}} \oplus (p-1, 1)_{\widetilde{\text{NS}}}. \quad (7.3c)$$

Note that if the initial boundary condition is of Neveu–Schwarz type, then the result of the flow is a Ramond type boundary condition and vice versa. We also identified the flows related to the flow (7.4) by the disorder line rule:

$$(r, p)_{\text{NS}} \longrightarrow (p - r, 1)_{\text{R}}, \quad (7.4a)$$

$$(r, p)_{\widetilde{\text{NS}}} \longrightarrow (p - r, 1)_{\text{R}}, \quad (7.4b)$$

$$(r, p)_{\text{R}} \longrightarrow (p - r, 1)_{\text{NS}} \oplus (p - r, 1)_{\widetilde{\text{NS}}}. \quad (7.4c)$$

2. For $\kappa < 0$:

(a) For $3 \leq s \leq p$

$$(1, s)_{\text{NS}} \longrightarrow (s - 2, 1)_{\widetilde{\text{NS}}}, \quad (7.5a)$$

$$(1, s)_{\widetilde{\text{NS}}} \longrightarrow (s - 2, 1)_{\text{NS}}, \quad (7.5b)$$

$$(1, s)_{\text{R}} \longrightarrow (s - 2, 1)_{\text{R}}. \quad (7.5c)$$

This again gives back the Fredenhagen flow (6.20). We found that the disorder line rule applies: we identified the flows

$$(r, s) \rightarrow (|r - s + 2| + 1, 1) \oplus (|r - s + 2| + 3, 1) \oplus \cdots \oplus (\min(\frac{s+r-3}{2p-(s+r)+1}, 1), 1). \quad (7.6)$$

In the Neveu–Schwarz case these flows, just like their ancestors, change the type of the boundary conditions. The comment given in case 1a is true here as well.

(b) For $s = 2$

$$(1, 2)_{\text{R}} \longrightarrow (1, 1)_{\text{NS}} \oplus (1, 1)_{\widetilde{\text{NS}}}. \quad (7.7)$$

This is another example for a flow starting from a Ramond boundary condition running to a Neveu–Schwarz one. The disorder line rule is consistent with the flows

$$(r, 2)_{\text{NS}} \longrightarrow (r, 1)_{\text{R}}, \quad (7.8a)$$

$$(r, 2)_{\widetilde{\text{NS}}} \longrightarrow (r, 1)_{\text{R}}, \quad (7.8b)$$

$$(r, 2)_{\text{R}} \longrightarrow (r, 1)_{\text{NS}} \oplus (r, 1)_{\widetilde{\text{NS}}}. \quad (7.8c)$$

It is interesting that despite the lack of a complete classification of consistent boundary states for p even, our results indicate the same rules for these cases. The only exception is the boundary condition corresponding to the supersymmetric $(\frac{p}{2}, \frac{p+2}{2})$ representation which could not be investigated directly by TCSA.

It is also interesting to note that via the symmetry transformation of the Kac table ($r \rightarrow p - r$, $s \rightarrow p + 2 - s$) the rules (7.2), (7.4) are mapped to the rules (7.6) and (7.8), respectively. This means that the two groups of rules ($\kappa < 0$, $\kappa > 0$) are not independent.

We note that although one can only approach and never reach the fixed point, the endpoints are $(r, 1)$ type boundary conditions that have no relevant supersymmetric perturbations, so it is reasonable to take our observations to be strong indications for the real result.

8 Conclusions

In this work we investigated the renormalisation group flows of boundary conditions in $N = 1$ superconformal minimal models. Starting from a pure Cardy-type boundary condition, the (supersymmetry preserving) perturbing operator $\hat{G}_{-1/2}\Phi_{1,3}$ induces a renormalisation group flow whose infrared fixed points are again superconformal invariant boundary conditions. As we have shown, the Fredenhagen rules [16] for boundary flows in general coset theories predict the IR fixed points of our flows. The predicted flows obey a product rule called disorder line rule [18].

In this paper we used the TCSA method to check the Fredenhagen rules. We found that these rules held in every case that we investigated. It is interesting to note that there are flows which go from a Neveu-Schwarz type boundary condition to a Ramond type, and vice versa. Finally, we showed that all the flows obey the disorder line rule.

Although for p even both these predictions and the description of boundary states are flawed by the presence of the supersymmetric representation, our analysis implies that a natural extension of the rules are valid for these models.

There are several possibilities for continuing this work. One of them is its extension to the study of the more complicated space of flows of non-Cardy type boundary conditions. Another possibility is to consider $N = 2$ models, which have direct relevance in string theory. However, although the TCSA analysis should be straightforward in principle, we expect too many states for reasonably high cuts, which can spoil the applicability of TCSA in practice. It would be interesting to include non-unitary models, too. The energies typically become complex in these models (like for ordinary minimal models, as reported in [10]), which makes the identification of the endpoint rather difficult.

Acknowledgement

I would like to thank my supervisor, Gábor Takács for his guidance, help and the interesting discussions. I am also grateful to Stefan Fredenhagen for his valuable remarks.

A Appendix

In the appendix we present the results of the TCSA for the first unitary models in detail. In the subsections we follow the classification of the flows given in section 7. In the tables the “level” entry indicates the level up to which the agreement between the character and the calculated degeneracy pattern in the IR holds. In the fourth field of every row the dimension of the truncated Hilbert space is shown. The last field contains the number of the corresponding figure.

In the figures collected at the end of the Appendix we plotted the energy levels against the dimensionless coupling parameter κ . In these figures the starting boundary condition is unprojected for the Neveu–Schwarz ones (i.e. $\text{NS} \oplus \widetilde{\text{NS}}$), so these flows go to unprojected NS or R boundary conditions. In figure 1(a) the energy itself is plotted, while in all the other figures we plotted the normalised energy $(\varepsilon - \varepsilon_0)/(\varepsilon_i - \varepsilon_0)$ for some appropriate i (usually 1).

A.1 First group of flows: $\kappa > 0$

A.1.1 Flows starting from b. c. (r, s) when $s \leq p - 1$

These flows are predicted by the Fredenhagen rules and our results agree with these predictions.

$$(r, s) \rightarrow (|s - r| + 1, 1) \oplus (|s - r| + 3, 1) \oplus \cdots \oplus (\min \binom{s+r-1}{2p-(s+r)-1}, 1)$$

model	flow	level	dim	fig.
SM(3, 5)	$(1, 2) \rightarrow (2, 1)$	11	302	1(c)
SM(4, 6)	$(1, 3) \rightarrow (3, 1)$	16	454	2(a)
	$(2, 2) \rightarrow (1, 1) \oplus (3, 1)$	17,15	536	2(b)
	$(1, 2) \rightarrow (2, 1)$	11	414	
SM(5, 7)	$(1, 3) \rightarrow (3, 1)$	13	388	
	$(2, 2) \rightarrow (1, 1) \oplus (3, 1)$	13,11	311	
	$(2, 4) \rightarrow (3, 1)$	12	601	3(b)
	$(1, 2) \rightarrow (2, 1)$	11	341	
	$(1, 4) \rightarrow (4, 1)$	7	357	3(c)
	$(2, 3) \rightarrow (2, 1) \oplus (4, 1)$	8,6	303	3(d)
SM(6, 8)	$(1, 3) \rightarrow (3, 1)$	14	396	
	$(1, 5) \rightarrow (5, 1)$	8	540	4(a)
	$(2, 2) \rightarrow (1, 1) \oplus (3, 1)$	13,11	316	
	$(2, 4) \rightarrow (3, 1) \oplus (5, 1)$	12,8	440	4(b)
	$(1, 2) \rightarrow (2, 1)$	10	344	
	$(1, 4) \rightarrow (4, 1)$	7	385	
	$(2, 3) \rightarrow (2, 1) \oplus (4, 1)$	8,6	318	
	$(2, 5) \rightarrow (4, 1)$	6	367	4(d)
	$(3, 2) \rightarrow (2, 1) \oplus (4, 1)$	9,8	317	4(e)

A.1.2 Flows starting from b. c. (r, s) when $s = p$

These flows are not predicted by the Fredenhagen rules. Based on the TCSA data we propose:

$$(r, p) \longrightarrow (p - r, 1)$$

model	flow	level	dim	fig.
SM(3, 5)	$(1, 3) \rightarrow (2, 1)$	6	407	1(b)
SM(4, 6)	$(1, 4) \rightarrow (3, 1)$	18	490	2(c)
SM(5, 7)	$(1, 5) \rightarrow (4, 1)$	7	298	3(a)
SM(6, 8)	$(1, 6) \rightarrow (5, 1)$	14	289	4(f)
	$(2, 6) \rightarrow (4, 1)$	7	426	4(c)

A.2 Second group of flows: $\kappa < 0$

A.2.1 Flows starting from b. c. (r, s) when $s \geq 3$

These flows are again covered by the Fredenhagen rules. The TCSA results verified these rules.

$$(r, s) \rightarrow (|r - s + 2| + 1, 1) \oplus (|r - s + 2| + 3, 1) \oplus \cdots \oplus (\min \binom{s+r-3}{2p-(s+r)+1}, 1)$$

model	flow	level	dim	fig.
SM(3, 5)	$(1, 3) \rightarrow (1, 1)$	12	407	1(b)
SM(4, 6)	$(1, 3) \rightarrow (1, 1)$	18	454	2(a)
	$(1, 4) \rightarrow (2, 1)$	10	490	2(c)
SM(5, 7)	$(1, 3) \rightarrow (1, 1)$	12	388	
	$(1, 5) \rightarrow (3, 1)$	14	298	3(a)
	$(2, 4) \rightarrow (1, 1) \oplus (3, 1)$	15,13	601	3(b)
	$(1, 4) \rightarrow (2, 1)$	9	357	3(c)
	$(2, 3) \rightarrow (2, 1)$	8	303	3(d)
SM(6, 8)	$(1, 3) \rightarrow (1, 1)$	14	396	
	$(1, 5) \rightarrow (3, 1)$	14	540	4(a)
	$(2, 4) \rightarrow (1, 1) \oplus (3, 1)$	13,11	440	4(b)
	$(2, 6) \rightarrow (3, 1) \oplus (5, 1)$	17,13	426	4(c)
	$(1, 6) \rightarrow (4, 1)$	9	289	4(f)
	$(1, 4) \rightarrow (2, 1)$	9	385	
	$(2, 3) \rightarrow (2, 1)$	7	318	
	$(2, 5) \rightarrow (2, 1) \oplus (4, 1)$	7,5	367	4(d)

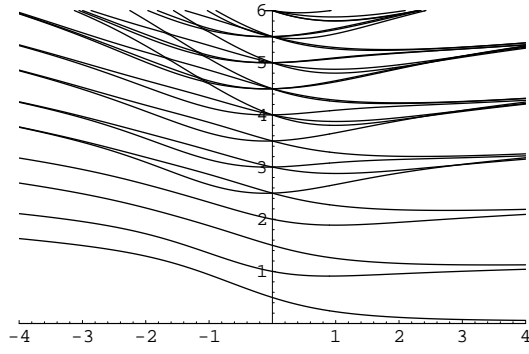
A.2.2 Flows starting from b. c. (r, s) when $s = 2$

Finally, we present the second type of exceptional (unpredicted) flows:

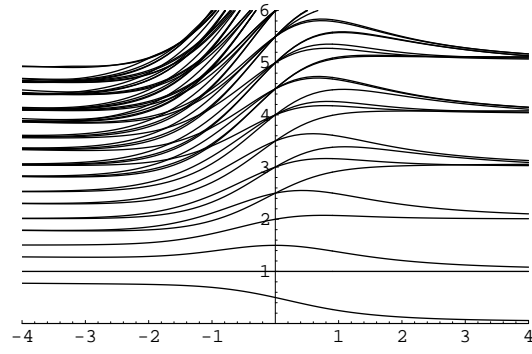
$$(r, 2) \longrightarrow (r, 1)$$

model	flow	level	dim	fig.
SM(3, 5)	$(1, 2) \rightarrow (1, 1)$	9	302	1(c)
SM(4, 6)	$(2, 2) \rightarrow (2, 1)$	9	536	2(b)
	$(1, 2) \rightarrow (1, 1)$	22	414	
SM(5, 7)	$(2, 2) \rightarrow (2, 1)$	7	311	
	$(1, 2) \rightarrow (1, 1)$	20	341	
SM(6, 8)	$(2, 2) \rightarrow (2, 1)$	7	316	
	$(1, 2) \rightarrow (1, 1)$	20	344	
	$(3, 2) \rightarrow (3, 1)$	16	317	4(e)

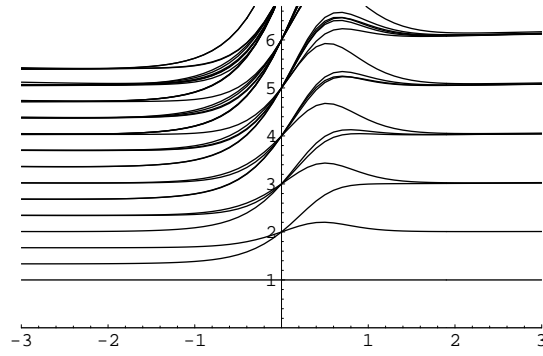
Figures



(a) Flows starting from b.c. (1, 3) in SM(3,5)

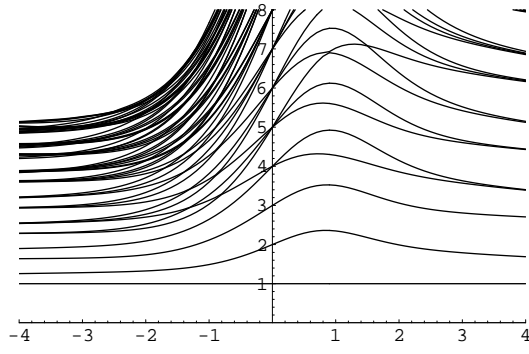


(b) Flows starting from b.c. (1, 3) in SM(3,5)

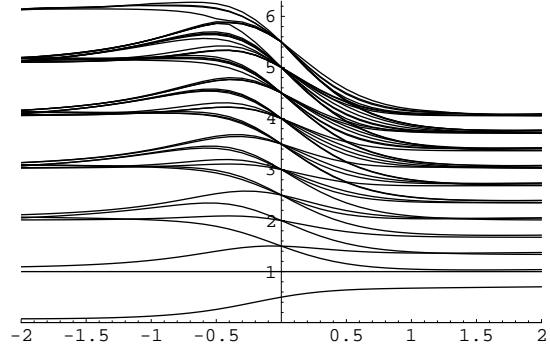


(c) Flows starting from b.c. (1, 2) in SM(3,5)

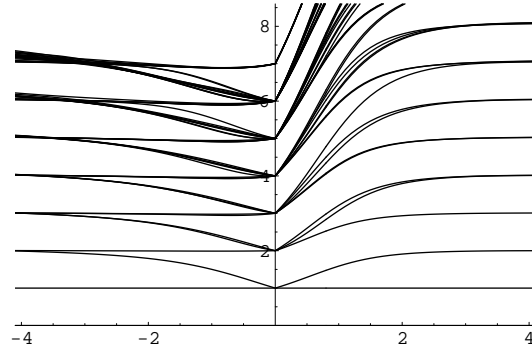
Figure 1: Flows in SM(3,5)



(a) Flows starting from b.c. (1, 3) in SM(4,6)

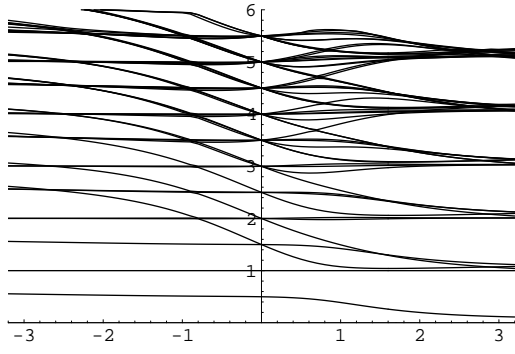


(b) Flows starting from b.c. (2, 2) in SM(4,6)

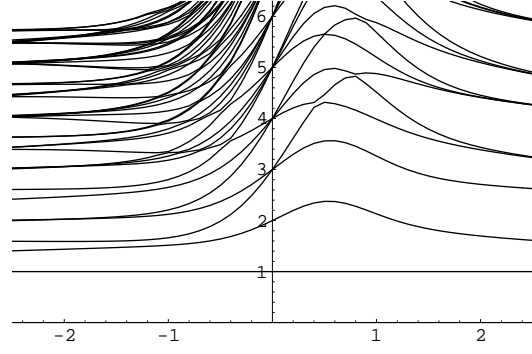


(c) Flows starting from b.c. (1, 4) in SM(4,6)

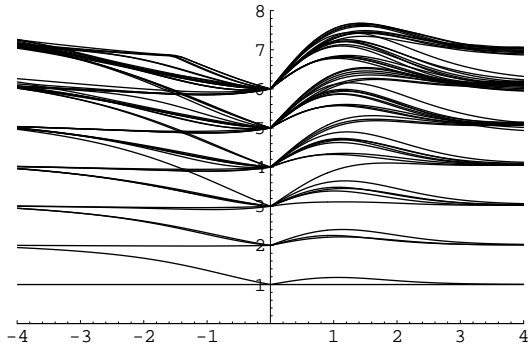
Figure 2: Flows in SM(4,6)



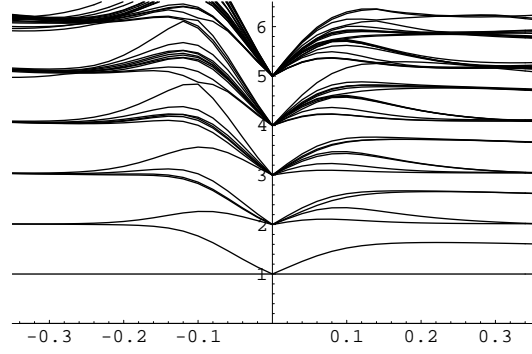
(a) Flows starting from b.c. (1, 5) in SM(5,7)



(b) Flows starting from b.c. (2, 4) in SM(5,7)

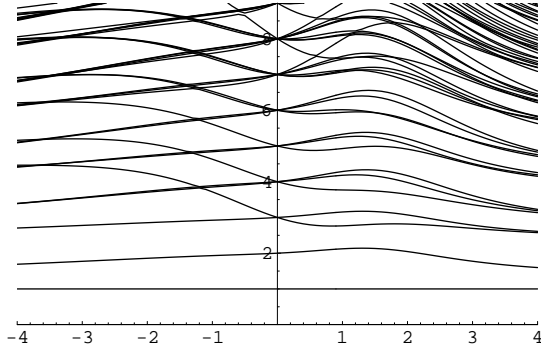


(c) Flows starting from b.c. (1, 4) in SM(5,7)

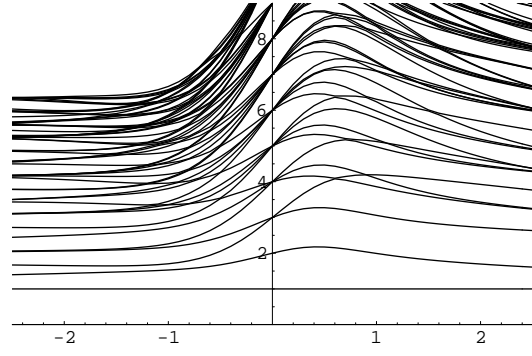


(d) Flows starting from b.c. (2, 3) in SM(5,7)

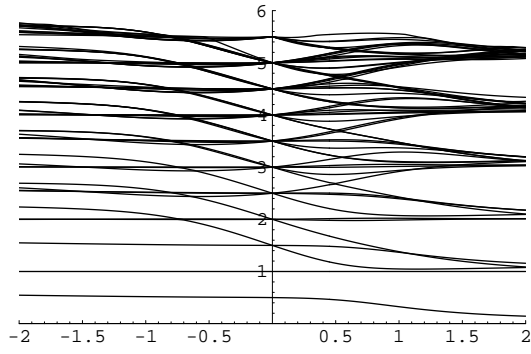
Figure 3: Flows in SM(5,7)



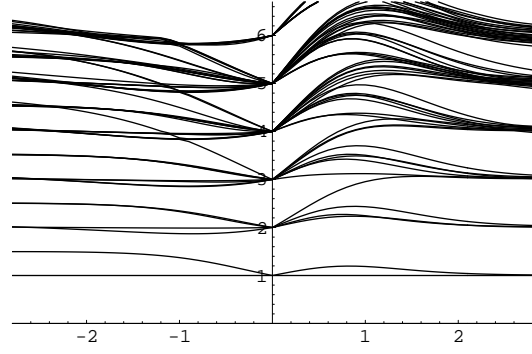
(a) Flows starting from b.c. (1, 5) in SM(6,8)



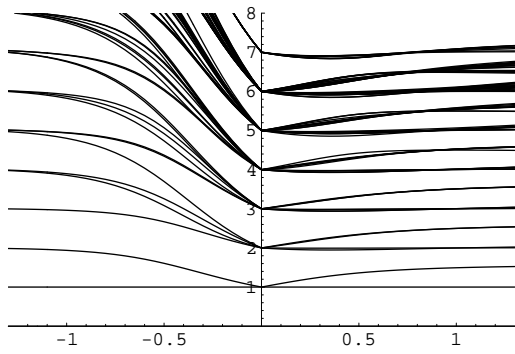
(b) Flows starting from b.c. (2, 4) in SM(6,8)



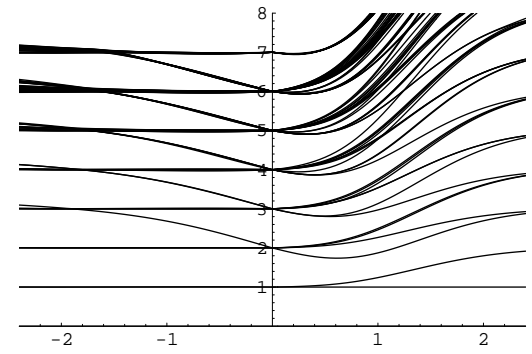
(c) Flows starting from b.c. (2, 6) in SM(6,8)



(d) Flows starting from b.c. (2, 5) in SM(6,8)



(e) Flows starting from b.c. (3, 2) in SM(6,8)



(f) Flows starting from b.c. (1, 6) in SM(6,8)

Figure 4: Flows in SM(6,8)

References

- [1] H. Saleur: *Lectures on Non Perturbative Field Theory and Quantum Impurity Problems*, `cond-mat/9812110`
- [2] C. Angelantonj, A. Sagnotti: *Open Strings*, *Phys. Rept.* **371** (2002) 1 (`hep-th/0204089`)
- [3] J. A. Harvey, D. Kutasov, E. J. Martinec: *On the relevance of tachyons*, `hep-th/0003101`
- [4] A. Recknagel, D. Roggenkamp, V. Schomerus: *On relevant boundary perturbations of unitary minimal models*, *Nucl. Phys.* **B558** (2000) 552 (`hep-th/0003110`)
- [5] P. Dorey, I. Runkel, R. Tateo, G. Watts: *g-function flow in perturbed boundary conformal field theories*, *Nucl. Phys.* **B578** (2000) 85 (`hep-th/9909216`)
- [6] F. Lesage, H. Saleur, P. Simonetti: *Boundary flows in minimal models*, *Phys. Lett.* **B427** (1998) 85 (`hep-th/9802061`)
- [7] K. Graham, I. Runkel, G. M. T. Watts: *Minimal model boundary flows and $c = 1$ CFT*, *Nucl. Phys.* **B608** (2001) 527 (`hep-th/0101187`)
- [8] K. Graham, I. Runkel, G. M. T. Watts: *Renormalisation group flows of boundary theories*, (`hep-th/0010082`)
- [9] V. P. Yurov, Al. B. Zamolodhikov: *Truncated conformal space approach to the scaling Lee-Yang model*, *Int. J. Mod. Phys.* **A5** (1990) 3221
- [10] P. Dorey, A. Pocklington, R. Tateo, G. Watts: *TBA and TCSA with boundaries and excited states*, *Nucl. Phys.* **B525** (1998) 641 (`hep-th/9712197`)
- [11] G. M. T. Watts: *Null vectors of the superconformal algebra: the Ramond sector*, *Nucl. Phys.* **B407** (1993) 213 (`hep-th/9306034`)
- [12] R. I. Nepomechie: *Consistent superconformal boundary states*, *J. Phys.* **A34** (2001) 6509 (`hep-th/0102010`)
- [13] N. Ishibashi: *The Boundary and Crosscap States in Conformal Field Theory*, *Mod. Phys. Lett* **A4** (1989) 251
- [14] J. L. Cardy: *Boundary conditions, fusion rules and the Verlinde formula*, *Nucl. Phys.* **B324** (1989) 581
- [15] P. Mathieu: *Integrability of perturbed superconformal minimal models*, *Nucl. Phys.* **B336** (1990) 338

- [16] S. Fredenhagen: *Organizing boundary RG flows*, *Nucl. Phys.* **B660** (2003) 436
([hep-th/0301229](#))
- [17] P. Goddard, A. Kent, D. I. Olive: *Unitary representations of the Virasoro and super-Virasoro algebras*, *Commun. Math. Phys.* **103** (1986) 105
- [18] K. Graham, G. M. T. Watts: *Defect Lines and Boundary Flows*, *JHEP* **0404**
(2004) 019 ([hep-th/0306167](#))
- [19] Ch. Ahn, Ch. Rim: *Boundary Flows in general Coset Theories*, *J. Phys.* **A32**
(1999) 2509 ([hep-th/9805101](#))